



## Landscaping of Entire Range of Non-covalent interactions in Theophylline monohydrate and anhydrous Theophylline through Hirshfeld surface analysis

By

Ahsan Ullah<sup>\*1</sup>, Muhammad Umair<sup>2</sup>, Muhammad Usama<sup>3\*</sup>, Tahir Abbas<sup>2</sup>, Muhammad Irfan<sup>5</sup>, Makkah Zaman<sup>6</sup>, Tahseen Anwer<sup>7</sup>, Muhammad Nouman Sarwar<sup>8</sup>, Jehanzaib Ahmed<sup>9</sup>, Muhammad Ali<sup>5</sup>

<sup>\*1</sup>Institute of Chemistry, The Islamia University of Bahawalpur, 63100 Bahawalpur, Pakistan

<sup>2,4</sup>Department of Chemistry, Kohat University of Science and Technology, Pakistan

<sup>3</sup>Department of Chemistry, University of Education, Lahore, Pakistan

<sup>5</sup>Institute of Chemical Sciences BZU, Multan, Pakistan

<sup>6</sup>Department of Chemistry, University of Malakand Chakdara, Pakistan

<sup>7,8</sup>Department of Chemistry, University of Agriculture Faisalabad, Punjab Pakistan

<sup>9</sup>Department of Chemistry, University of Lahore, Pakistan



### Article History

Received: 25/12/2024

Accepted: 28/12/2024

Published: 31/12/2024

### Vol – 3 Issue –12

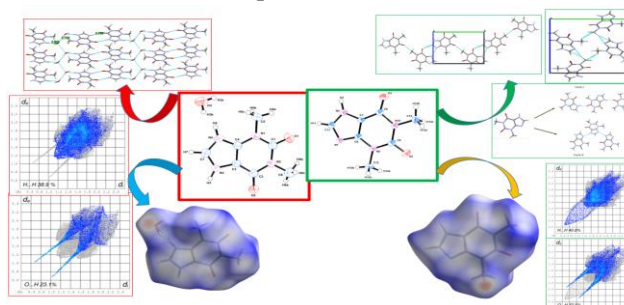
PP: - 198-207

DOI:10.5281/zenodo.14582360

### Abstract

*Theophylline monohydrate and polymorphs of anhydrous theophylline are being compared. Crystallographic data was obtained using the Cambridge structural data source. In this investigation, 1,3-Dimethyl-3,7-dihydro-1H-purine-2,6-dione monohydrate (Ref-code: THEOPH) and 1,3-Dimethyl-3,7-dihydro-1H-purine-2,6-dione (Ref-code: BAPLOT) are chosen. Hirshfeld surface tools were used to visualize the different types of intermolecular interactions throughout the crystal range of theophylline monohydrate and polymorphs of anhydrous theophylline. The fundamental distinction between theophylline monohydrate and anhydrous theophylline appears to be the N—H...O bond dimer. Some other weak interactions distinguish the molecular packing. After the creation of two N—H...O hydrogen bonds, the theophylline dimers that make up the theophylline monohydrate structure are joined by an inversion center. Because of these dimers and having a large percentage of hydrogen and oxygen interactions theophylline monohydrate has a distinctive structure and better tabletability than anhydrous theophylline.*

### Graphical Abstract



### Introduction

Materials science tetrahedron (MST) tells us about the inter dependent relationship between the process of development of the drugs, their structure and properties. MST aspects the form of scientific foundations for the development and design of new drugs products in pharmaceutical science. MST has many applications in drugs development and pharmaceutical research. Most efficient, coherent and collaborative research

conduct by pharmaceutical science community[1]. Mechanical and physicochemical properties are more effected by crystal structure than a molecular structure. Therefore crystal engineering in materials science research play an important role[2]. These mechanical properties of the materials are related with tableting[3] performance of powders of the pharmaceutical drugs[4]. As a result the tablet ability of the drugs can be determine by Hirshfeld surface analysis[5] on

the basis of different types of interactions in the crystal structure.

Theophylline, a medication that was first identified in 1888, was initially extracted from sources such as tea leaves, coffee, and chocolate [6]. It has been employed in the pharmaceutical sector and for disease treatment purposes since 1992. "THEO" is a shortened form of theophylline. THEO is a potent bronchodilator and broncho spasmolytic agent, primarily employed for managing bronchial asthma. It is included in both the United States Pharmacopeia and European Pharmacopeia, and pharmaceutical research continues to place significant emphasis on studying this drug and its characteristics. THEO serves as a model compound for investigating hydrate formation and polymorphism.

If the water molecules are present in the crystal lattice often lead to different crystal structure, which is probability to impact on its pharmaceutical importance [7]. It was found that some hydrate exhibit better properties than its anhydrate form [7]. It is important to explore crystal hydration have benefits or nor for general applicability. Because of structural characteristics that result in several slide mechanisms, theophylline anhydrate (THa) was demonstrated to be extremely flexible and to have outstanding tablet ability [8]. It has been observed that theophylline monohydrate (THm) [8, 9] performs even better when it comes to tableting than THa [10]. Though the authors did not mention it, it is likely that the THm in the earlier research had a different particle size and shape from the THa since it was crystallized from water. Therefore, it is still unknown whether THm's better tableting ability resulted from variations in mechanical characteristics or from distinct specific features [11].

The fact that some crystals are supramolecular systems should not be overlooked. Subsequently, the smallest structural units produced by the intermolecular interactions, supramolecular synthons, may be used to characterize their structural characteristics. In supramolecular architecture, the combinations of several synthons is important for crystal engineering [12, 13]. Understanding intermolecular interactions and using them to the construction of new molecules with targeted designs and enhanced characteristics is the primary goal of crystal engineering. However, a significant challenge is the multiplicity of interactions that govern crystal formations [14].

X-ray crystallography was used to analyze the structural characteristics of the polymorphous of theophylline [13]. Given the significance of the aforementioned, the primary objective of this study is to conduct a thorough comparative analysis of the structural variations and similarities among all finasterides currently in use. This analysis will encompass both qualitative and quantitative exploration of the nature of intermolecular interactions and crystal packing behavior by using Hirshfeld surface analysis.

Examine the molecular interactions within a crystal structure using a technique called Hirshfeld surface analysis [5]. The Hirshfeld surface proved to be a remarkable discovery in this context and garnered significant attention because of its

distinct properties for investigating the intermolecular interactions within crystals.

Hirshfeld surfaces are employed for a comprehensive examination of the interactions between chemical compounds and the arrangement of molecules within a crystal. It is possible to create a fingerprint plot by analyzing the distances from the surface to the closest atoms either outside or inside the surface [15].

Within the realm of crystals, the investigation of intermolecular interactions and the visualization of these phenomena are highly prevalent practices. Utilizing these visualization tools, one can generate fingerprint plots that depict the interactions between pairs of chemical species. This method allows for the identification of various types of interactions, including van der Waals contacts, hydrogen bonding (such as C—H... $\pi$ ), and  $\pi$ ... $\pi$  stacking, through the analysis of fingerprint plots.

The distances from atoms on the Hirshfeld surface to the nearest atoms within the surface (di) and to the atoms outside of the surface (de) are calculated to generate 2-D fingerprint plots. These fingerprint plots encode information about the nature and types of interactions within molecules found in crystal structures that consist of more than one molecule [16].

In the fingerprint plots, various types of contacts are depicted, with red and blue colors signifying longer and closer contacts, respectively, while green represents neither close nor distant contacts. Additionally, the spikes, wider regions, and wing-shaped areas within the plots convey both the types and the extent of these interactions.

## Method and Materials

Crystallization is a purification and separation technique employed for the manufacture of a variety of substances, from bulk industrial chemicals to pharmaceuticals and specialized chemicals. Depending on the amount of the Sample, several procedures for crystallization such as evaporation, cooling, diffusion, sublimation, and vapor diffusion are used. Without any further purification, the aforementioned chemical theophylline (3,7-dihydro-1,3-dimethyl-1H-purine-2,6-dione) was employed. After being crushed in a pestle mortar with ethanol added drop by drop, 0.4g of theophylline's white powder was immersed in 10 ml of ethanol and agitated for 3–4 hours. The mixture was slowly evaporated to produce crystals at room temperature. Theophylline crystals in the form of clear, needle-shaped formations were produced in a week. Olympus microscope chooses the crystal for x-ray diffraction investigation. With the help of a micro-focus source and a graphite monochromatized Mo k (0.71073) source of radiation on a Bruker-D8 Venture diffractometer equipped with a photon Sensor PHOTON II, information of single crystal was collected at 298 K. Rest of the structures of the polymorphous of theophylline was taken from the Cambridge Crystallographic Data Center (CCDC) [17].

- 2,6-dimethyl-1,3,7-dihydro-1H-purine monohydrate (Ref-code:THEOPH).
- The compound 1,3-Dimethyl-3,7-dihydro-1H-purine-2,6-dione (ref-code: BAPLOT).

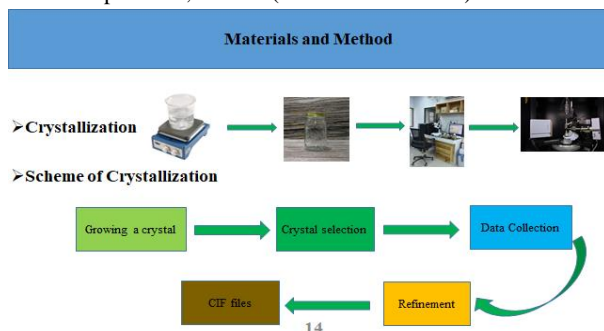


Figure 1 Scheme of laboratory experiment

### Crystal structural Analysis

CIF files of Anhydrous theophylline and theophylline anhydrate (Reference code: BAPLOT02) and Theophylline monohydrate ( Reference code: THEOPH04 ) were downloaded. Mercury software and Crystal Explorer [18] were used to analyze the CIFs that were retrieved from the Cambridge Structural Database.

### Crystal packing of Theophylline Monohydrate

Figure 3 shows a unit cell of theophylline monohydrate at 273K. Theophylline monohydrate has 4 molecules per unit cell, which is found in a monoclinic with space group P21/n. The structure of theophylline monohydrate contains theophylline dimers, which are joined by the inversion Centre. This outcome is the product of two N—H...O hydrogen bonds formed between N3 and H3, and a single hydrogen bond created among N4—H4...O3 with N...H bond distance 0.860(4) Å, H...O bond distance 1.91(2) Å and N...O bond distance 2.76(10) Å. Due to the exposure of the extremely basic nitrogen atom N3, which is peculiar to this dimerization in theophylline's crystal structure, it is thought to be crucial in the production of hydrates. In the form of a layer, dimers are present in Theophylline monohydrate along a-axis. Between these layers, there is no hydrogen bond. 2024/12/26. Water molecule channels separate theophylline layers along the b-axis, which interact with THEO molecules through a hydrogen connection to N3 as seen in Figure 4.

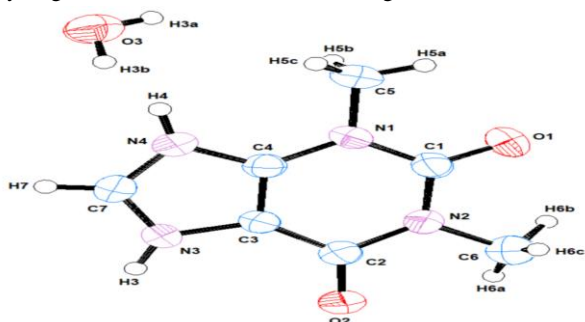


Figure 2 A 50% probability thermal ellipsoid diagram of theophylline monohydrate displays the arrangement of hydrogen and non-hydrogen atoms.

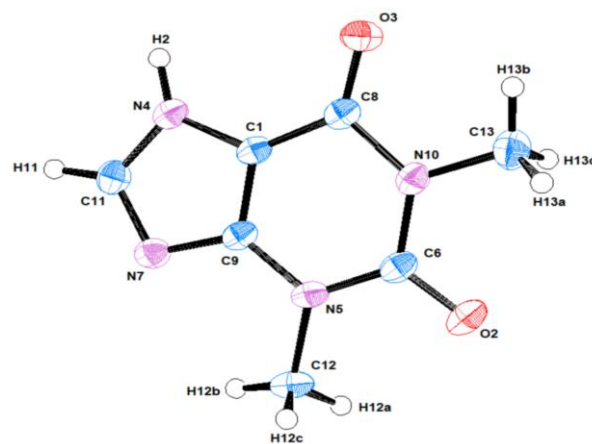


Figure 3 The numbering method of hydrogen and non-hydrogen atoms is represented by a thermal ellipsoid diagram of anhydrous theophylline drawn with 50% probability.

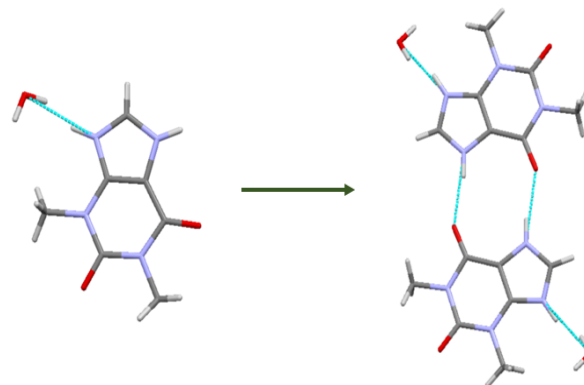


Figure 4 Theophylline monohydrate's hydrogen bonding

Through hydrogen bonding among the oxygen atom of the benzene ring and the nitrogen atom of the purine ring, molecules are stacked on top of one another and joined in an unending chain.

### Crystal Packing of Anhydrous Theophylline

Figure 5 shows the anhydrous theophylline cell units around 273K, 298K, and 290K. The space groups P21/c, which include 4 and 8 molecules per unit cell, and Pn, which have only two molecules per unit cell, make up the monoclinic structure of the single cell of anhydrous theophylline. By polymorphism, anhydrous theophylline can be found in orthorhombic with a space group Pna21 and four molecules for each cell. When Form I of anhydrous theophylline crystallized, an orthorhombic cell unit having the space group Pna21 and 4 molecules within an asymmetric unit (Z=4) is present. The theophylline structure itself is thinner and has a methyl group of THEO in a plane with a purine ring. The NH group of one molecule's 5-membered ring (N4-H4), acted as the donor, and the carbonyl group of another molecule's 6-membered rings, acted as the acceptor, establishing H-bonds. As a result, functional groups on the compound's other ends are linked, which causes the components to form H-bond chains with one another as pearls on a thread in the (201) and (-201), as seen in Figure 6. The hydrogen-linked chains'

ability to accumulate molecules on top of one another is known as the  $\pi \cdots \pi$ -stack. As a result, the arrangement forms stack levels with the subsequent levels being connected by  $2_1$  screw axes. Anhydrous theophylline became crystallized and re-examined in state II to enable analysis. A second orthorhombic cell unit with an identical space group Pna21 and plane THEO components as in form I makes these 2 polymorphisms of the similar space class an illustration of stacking polymorphism in diagram 4. There is just one major H-bond in both forms I and II. similar to Form II, I only display a single H-bond however it forms among the N4-H4 of one five-membered circle and the N3 of second. As seen in Figure 6(III), H-bonded networks take on an irregular structure as a result of a variety of H-bonds. Due to the different nature of hydrogen bond molecules in a zig-zag manner shown in Figure 6(III) Chains of substances encapsulating b-glide planes are not as planar as type I. H-bonding causes molecules to pile on top of one another and become linked in endless chains, creating layers along the b-axis [19].

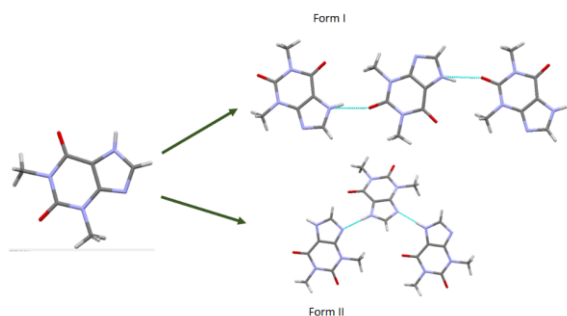
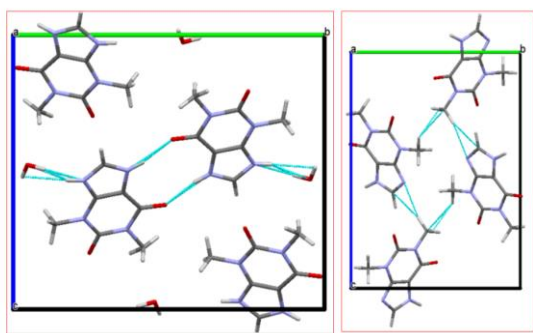
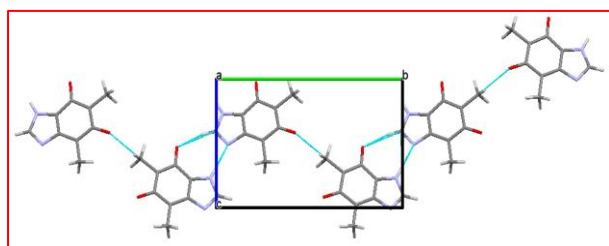


Figure 5 Hydrogen bonding of theophylline anhydrate form I and II



(I) (II)



(III)

Figure 6 .Theophylline monohydrate and anhydrous theophylline's crystal arrangement packing:

- (I) The inverted center for theophylline monohydrate with theophylline dimers along its a-axis at 273 K
- (II) (II) Anhydrous theophylline circle synthon polymorphs around its a-axis at 298 K
- (III) A-axis zigzag motif at 290K.

**Theophylline monohydrate has better tablet ability and flexibility compared to theophylline anhydrate stems from its crystal structure**

It is helpful to compare the crystal structures of theophylline monohydrate with dehydrated theophylline providing structural understanding of theophylline monohydrate's superior tablet ability and flexibility. The slip mechanism causes plastic deformation. Slip planes are examined by visual inspections of crystal packing or attachment energy. Attachment energy means energy is released when a crystal face grows by attaching new layers of molecules. Figure 6 illustrates the formation of rigid V-shaped hydrogen-bonded columns by anhydrous theophylline. Hydrogen bonds allow molecules to be layered on top of one another to create flat layers. When under stress, THa responds by easily deforming plastically, which is made possible by the slipping of stacking layers and improves stability. Theophylline monohydrate has a greater tablet ability as compared to anhydrous theophylline because of its larger bound area and weaker bonding. weak hydrogen interactions created among dimers in comparison to the two theophylline and water molecules. In dimers, the bond distance between N and O is 2.92Å, and the bond distance between two theophylline molecules (N-O) is 2.76Å. By hydrogen bonding, the molecules can be layered on top of one another to create the ladder-like layer in Figure 7. By weak N—H—O hydrogen interactions that overcome plastic deformation, hard ladders can be deformed along the <1 0 0> axes when under stress [7].

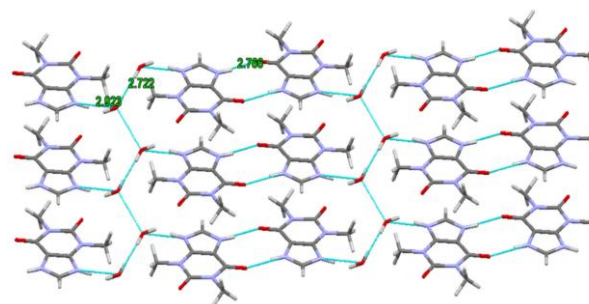


Figure 7. Theophylline monohydrate Crystal struc

## Experimental Details

**Table.1.** Crystal data of theophylline monohydrate

Crystal data	
Chemical formula	C <sub>7</sub> H <sub>8</sub> N <sub>2</sub> O <sub>2</sub> · H <sub>2</sub> O
<i>M</i> <sub>r</sub>	199.19
Crystal system, space group	Monoclinic, <i>P2<sub>1</sub>/n</i>
Temperature (K)	273
<i>a</i> , <i>b</i> , <i>c</i> (Å)	4.4814 (3), 15.3864 (10), 13.2752 (9)
<i>b</i> (°)	98.555 (2)
<i>V</i> (Å <sup>3</sup> )	905.17 (10)
<i>Z</i>	4
Radiation type	Mo <i>K</i> α
<i>m</i> (mm <sup>-1</sup> )	0.12
Crystal size (mm)	0.37 × 0.25 × 0.12
Data collection	
Diffractometer	Bruker D8 Venture with PHOTON II detector
Absorption correction	—
No. of measured, independent and observed [ <i>I</i> > 2σ( <i>I</i> )] reflections	5724, 1751, 1226
<i>R</i> <sub>int</sub>	0.048
(sin <i>q</i> / <i>l</i> ) <sub>max</sub> (Å <sup>-1</sup> )	0.625
Refinement	
<i>R</i> [ <i>F</i> <sup>2</sup> > 2σ( <i>F</i> <sup>2</sup> )], <i>wR</i> [ <i>F</i> <sup>2</sup> ], <i>S</i>	0.073, 0.234, 1.09
No. of reflections	1751
No. of parameters	138
H-atom treatment	H atoms treated by a mixture of independent and constrained refinement
<i>ρ</i> <sub>max</sub> , <i>ρ</i> <sub>min</sub> (e Å <sup>-3</sup> )	0.31, -0.74

**Table.2.** Crystal data of anhydrous theophylline

Crystal data		CCDC Code: BAPLOT03	CCDC Code: BAPLOT08
Chemical formula	C <sub>7</sub> H <sub>8</sub> N <sub>2</sub> O <sub>2</sub>	C <sub>7</sub> H <sub>8</sub> N <sub>2</sub> O <sub>2</sub>	C <sub>7</sub> H <sub>8</sub> N <sub>2</sub> O <sub>2</sub>
<i>M</i> <sub>r</sub>	180.17	180.17	180.17
Crystal system, space group	Monoclinic, <i>P2<sub>1</sub>/c</i>	Monoclinic, <i>P2<sub>1</sub>/c</i>	Monoclinic, <i>P2<sub>1</sub>/c</i>
Temperature (K)	299	298	298
<i>a</i> , <i>b</i> , <i>c</i> (Å)	7.8935 (6), 12.9087 (7), 15.9055 (8)	4.5310 (7), 11.5783 (1), 15.7188 (2)	4.5310 (7), 11.5783 (1), 15.7188 (2)
<i>b</i> (°)	104.214 (5)	93.69 (1)	93.69 (1)
<i>V</i> (Å <sup>3</sup> )	1571.07 (17)	822.9	822.9
<i>Z</i>	8	4	4
Radiation type	Mo <i>K</i> α	Mo <i>K</i> α	Mo <i>K</i> α
<i>m</i> (mm <sup>-1</sup> )	0.12	0.10	0.10
Crystal size (mm)	0.35 × 0.29 × 0.04	0.32 × 0.25 × 0.05	0.32 × 0.25 × 0.05
Data collection			
Diffractometer	Bruker–Nonius KappaCCD	Bruker–Nonius KappaCCD	Bruker–Nonius KappaCCD
Absorption correction	Multi-scan (SADABS, Sheldrick, 2003)	Multi-scan (SADABS, Sheldrick, 2003)	Multi-scan (SADABS, Sheldrick, 2003)
<i>T</i> <sub>min</sub> , <i>T</i> <sub>max</sub>	0.863, 0.995	0.823, 0.985	0.823, 0.985
No. of measured, independent and observed [ <i>I</i> > 2σ( <i>I</i> )] reflections	19027, 3074, 1972		
<i>R</i> <sub>int</sub>	0.058		
(sin <i>q</i> / <i>l</i> ) <sub>max</sub> (Å <sup>-1</sup> )	0.617		
Refinement			
<i>R</i> [ <i>F</i> <sup>2</sup> > 2σ( <i>F</i> <sup>2</sup> )], <i>wR</i> [ <i>F</i> <sup>2</sup> ], <i>S</i>	0.048, 0.129, 1.05		
No. of reflections	3074		

**Table.3.** Crystal data anhydrous theophylline

Crystal data		CCDC Code: BAPLOT06	CCDC Code: BAPLOT09
Chemical formula	C <sub>7</sub> H <sub>8</sub> N <sub>2</sub> O <sub>2</sub>	C <sub>7</sub> H <sub>8</sub> N <sub>2</sub> O <sub>2</sub>	C <sub>7</sub> H <sub>8</sub> N <sub>2</sub> O <sub>2</sub>
<i>M</i> <sub>r</sub>	180.17	180.17	180.17
Crystal system, space group	Orthorhombic, <i>Pna2<sub>1</sub></i>	Monoclinic, <i>Pn</i>	Monoclinic, <i>Pn</i>
Temperature (K)	150	290	290
<i>a</i> , <i>b</i> , <i>c</i> (Å)	24.3625 (2), 3.7781 (1), 8.4798 (1)	3.8744 (4), 12.8898 (9), 8.1167 (6)	3.8744 (4), 12.8898 (9), 8.1167 (6)
<i>V</i> (Å <sup>3</sup> )	780.51 (2)	400.40 (5)	400.40 (5)
<i>Z</i>	4	2	2
Radiation type	Mo <i>K</i> α	Mo <i>K</i> α	Mo <i>K</i> α
<i>m</i> (mm <sup>-1</sup> )	0.12	0.11	0.11
Crystal size (mm)	0.82 × 0.43 × 0.25	0.25 × 0.23 × 0.18	0.25 × 0.23 × 0.18
Data collection			
Diffractometer	Bruker APEX-II CCD	SuperNova, Dual, Cu at zero, Atlas	SuperNova, Dual, Cu at zero, Atlas
Absorption correction	—		
No. of measured, independent and observed [ <i>I</i> > 2σ( <i>I</i> )] reflections	8913, 8913, 8396	2386, 1499, 1168	2386, 1499, 1168
<i>R</i> <sub>int</sub>	0.045	0.024	0.024
(sin <i>q</i> / <i>l</i> ) <sub>max</sub> (Å <sup>-1</sup> )	1.111		
Refinement			
<i>R</i> [ <i>F</i> <sup>2</sup> > 2σ( <i>F</i> <sup>2</sup> )], <i>wR</i> [ <i>F</i> <sup>2</sup> ], <i>S</i>	0.049, 0.128, 1.30	0.063, 0.179, 1.07	0.063, 0.179, 1.07
No. of reflections	8913	1499	1499
No. of parameters	150	121	121
No. of restraints	9	2	2
H-atom treatment	All H-atom parameters refined	H-atom parameters constrained	H-atom parameters constrained
<i>ρ</i> <sub>max</sub> , <i>ρ</i> <sub>min</sub> (e Å <sup>-3</sup> )	0.62, -0.37	0.35, -0.26	0.35, -0.26
Absolute structure	Flack <i>x</i> determined using 3642 quotients [( <i>I</i> <sup>+</sup> - <i>I</i> <sup>-</sup> )/( <i>I</i> <sup>+</sup> + <i>I</i> <sup>-</sup> )] (Parsons, Flack and Wagner, Acta Cryst. B69 (2013) 249-259).	Flack <i>x</i> determined using 383 quotients [( <i>I</i> <sup>+</sup> - <i>I</i> <sup>-</sup> )/( <i>I</i> <sup>+</sup> + <i>I</i> <sup>-</sup> )] (Parsons and Flack (2004), Acta Cryst. A60, s61).	Flack <i>x</i> determined using 383 quotients [( <i>I</i> <sup>+</sup> - <i>I</i> <sup>-</sup> )/( <i>I</i> <sup>+</sup> + <i>I</i> <sup>-</sup> )] (Parsons and Flack (2004), Acta Cryst. A60, s61).
Absolute structure parameter	0.00 (12)	-2.1 (10)	-2.1 (10)

### Hirshfeld Surface Analysis and Fingerprint Plots

Hirshfeld surface analysis serves as a useful approach for evaluating and contrasting interactions among molecules that affect crystal packing. The molecular surfaces with weighted electron densities enable the identification of specific interactions. Such analysis is used for analyzing different types of inter-molecular interactions in crystal structure. It provides a non-overlapping and uniform surface [20]. Hirshfeld surface analysis illustrates both the type and extent of inter-molecular interaction within a super-molecular assemblage of anhydrous theophylline and theophylline monohydrate. The color range indicates the frequency of contact prevalence. The reddish color signifies less contact than the aggregate of van der Waal's radius of two atoms resulting in a negative value. Blue color signifies stronger connections whereas white signifies interactions near Van der Waal's boundaries and white represents interactions towards Van der Waal's radius. Figure 8 shows theophylline monohydrate's Hirshfeld surface map, which shows the presence of stronger intermolecular interactions and is shown in red N3—H3...O2, N4—H4...O3.

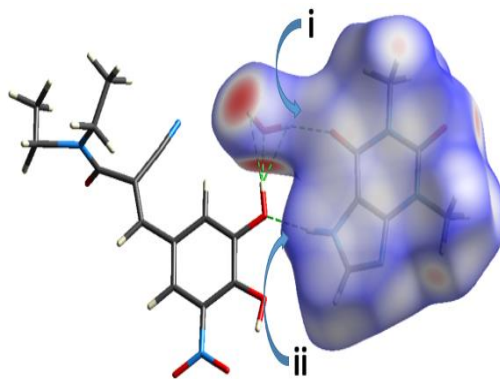


**Figure 8. Theophylline monohydrate Hirshfeld surface interacting with adjacent molecules at 273K**

Both the interactions between the oxygen molecules in water molecules and the interactions between N3—H3•••O2 and N4—H4•••O3 are highly strong. Theophylline monohydrate forms a dimer, and the water molecule present in theophylline monohydrate also forms a dimer and serves a crucial function in stabilizing the crystal structure, representing the strong interaction sides of the drug with arrows. Although N—H•••O provides 32.5% of theophylline monohydrate as observed in fingerprint graphs, theophylline monohydrate has greater flexibility as well as tablet ability.

Fingerprint graphs obtained from Crystal Explorer were used to investigate a 2-D depiction of Hirshfeld's analysis of anhydrous theophylline and theophylline monohydrate. The fingerprint plot is a 2-D graph that highlights specific intermolecular associations in a single crystal to extract superior information regarding molecular interactions. The quantifiable percentage of several types of interactions such as H-H, O-H, C-H, O-O and N-H was obtained. These many molecular interactions, particularly those that contribute the most percentage-wise, are crucial for stabilizing the crystal structure. CrystalExplorer17 [18] is used to map the fingerprint graphs of theophylline monohydrate and polymorphs of theophylline anhydrate. The framework of H-H and O-H associations plays an important role in crystal structure stabilization. Theophylline monohydrate has a percentage of H-H interaction of 40.9% and an O-H interaction of 32.5%. C-H interaction accounts for 10.0% of theophylline monohydrate. Other interactions present in theophylline monohydrate include N-C, N-N, O-N, and C-C with the lowest percentages of 1.2%, 1.8%, 2.2%, and 3.6%, respectively. H-H and O-H connections of H<sub>2</sub>O molecules contribute 65.8% and 27.2%, respectively to theophylline monohydrate.

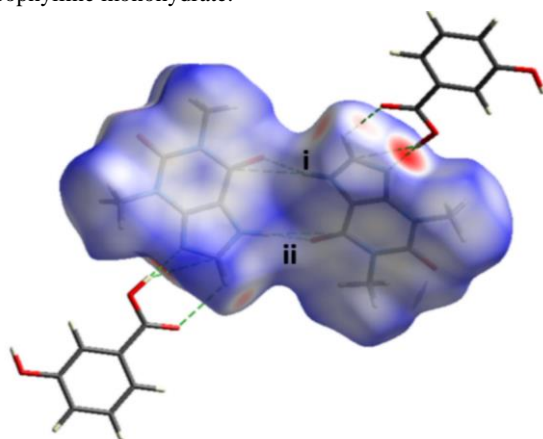


**Figure 9. Theophylline monohydrate Hirshfeld surface interacting with surrounding molecules at 298 K. Symmetry Codes: (i) -x, -y+1, -z; (ii) -x+3, -y+2, -z+1**

In anhydrous theophylline, the bonds between N<sub>4</sub>—H<sub>4</sub>•••O<sub>3</sub><sup>i</sup> and N<sub>8</sub>—H<sub>8</sub>•••O<sub>1</sub><sup>i</sup> are particularly strong. The percentages of various types of interactions in anhydrous theophylline vary. The average percentage of O-H interaction in theophylline

monohydrate is 32.5% while in anhydrous theophylline is 23.1%, 26.8%, and 27.6% among various anhydrous theophylline polymorphs as illustrated in figures 10 and 14. We may observe a change in the percentage of interactions between theophylline monohydrate and theophylline anhydrate.

**Table Error! No text of specified style in document.. H-bond geometry (Å, °) for anhydrous theophylline.**

D—H•••A	D—H	H•••A	D•••A	D—H•••A
N4—H4•••O3 <sup>i</sup>	0.86	1.92	2.753 (2)	163
N8—H8•••O1 <sup>i</sup>	0.86	1.94	2.782 (2)	165

Symmetry code: (i) -x, -y, -z+1.

### 1.1 Intermolecular Interaction

To investigate the interaction between the atoms in the crystal structure of theophylline and theophylline monohydrate, the 3D Hirshfeld surface and 2D fingerprint plot were created. Crystals were examined by Hirshfeld. Hirshfeld Figure 9 A, B, C, D, E, and F, respectively, depict surfaces of theophylline monohydrate mapped with d<sub>norm</sub>, di, de, shape index, curvedness, and fragment patch.

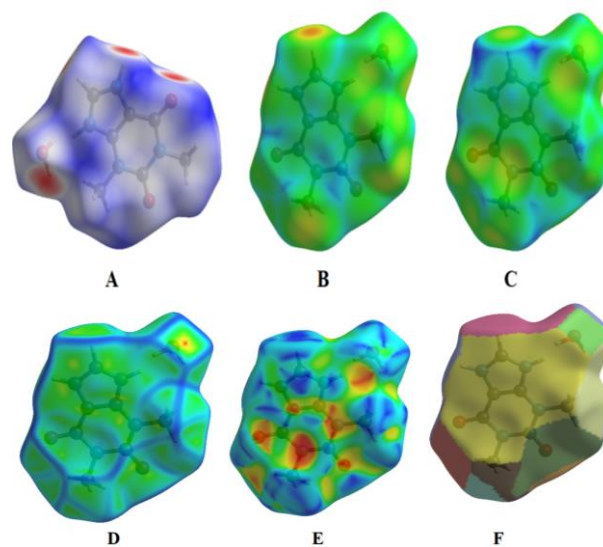


**Figure 10. Hirshfeld surface for Theophylline monohydrate mapped with d<sub>norm</sub>(A), di (B), de (C), shape index (D) curvedness (E), Fragment patch (F).**

Because of the strong hydrogen connections between OH and the Hirshfeld surface, the d<sub>norm</sub> surface exhibits a red color in some spots, indicating a significant interaction with the neighboring molecules. The bond length between O and H is 1.91(2) Å

In Hirshfeld surface analysis shape index is one of the main future that gives the identification of complementarity between the molecules in crystal packing [21]. Different colors in the form of spots on the surface of the shape index show intermolecular areas of complementarity. Concave regions of atoms and molecules stacked above one another

may be seen in the red areas. Blue-marked patches display a convex area that denotes the molecule's ring structure within the crystal surface.

Figure 10 displays the molecules' curvature. Low curvedness values on the surface relate to flat disc-shaped regions, whereas high curvedness values correspond to sharply edged curvatures that occasionally trend to the surface, demonstrating the interaction of nearby molecules. Blue outline separating flat patches indicates  $\pi$ - $\pi$  stacking interactions.

Information about the type of intermolecular contact between atoms is provided by a 2-D fingerprint image and represent major and minor intermolecular connection in the entire crystal structure[22].

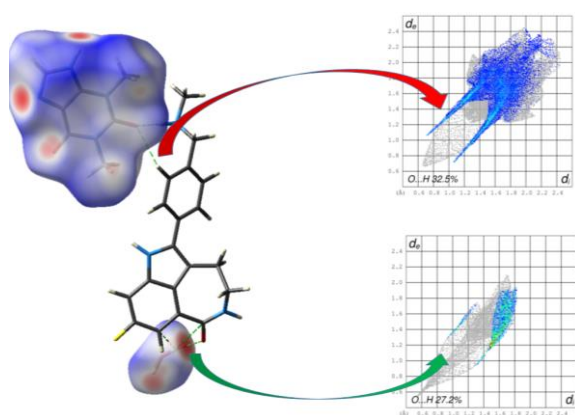


Figure 11. Landscape of theophylline monohydrate intermolecular interactions displaying O...H contact and water molecule O...H interaction

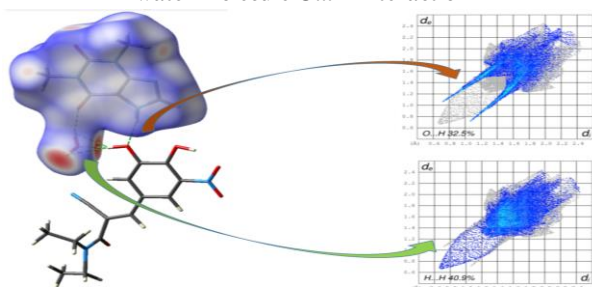


Figure 12. Theophylline monohydrate intermolecular interactions landscape exhibiting O...H and H...H interactions.

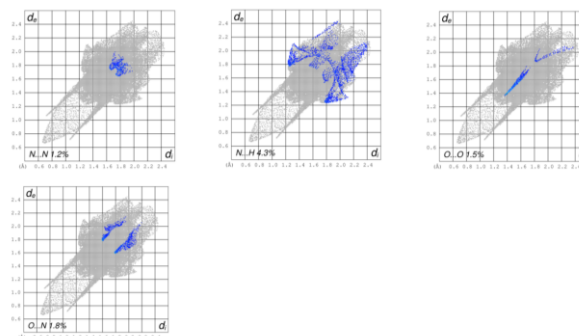
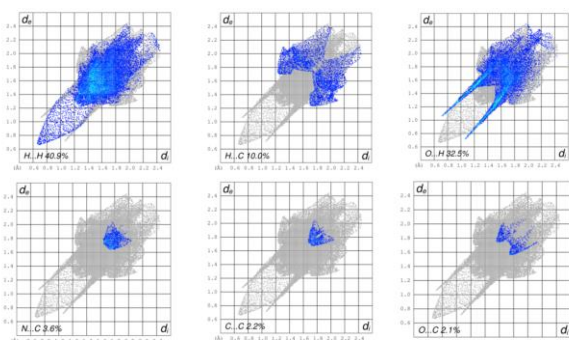


Figure 13. Theophylline monohydrate two-dimensional fingerprint plots with various levels of interaction.

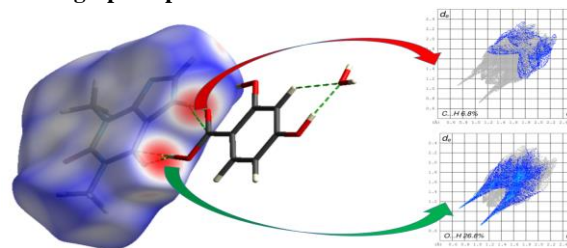


Figure 14. Anhydrous theophylline intermolecular interactions landscaping demonstrating C...H and O...H interactions.

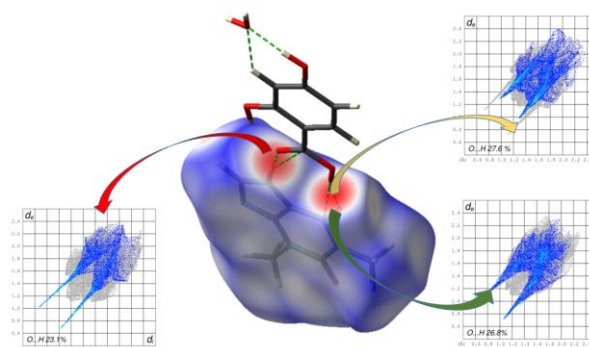
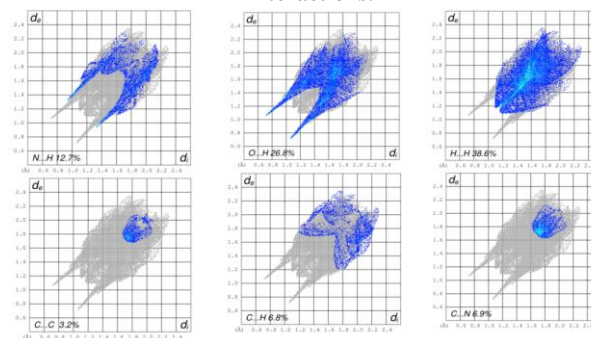


Figure 15. Anhydrous theophylline intermolecular interactions landscaping demonstrating C...H and O...H interactions.



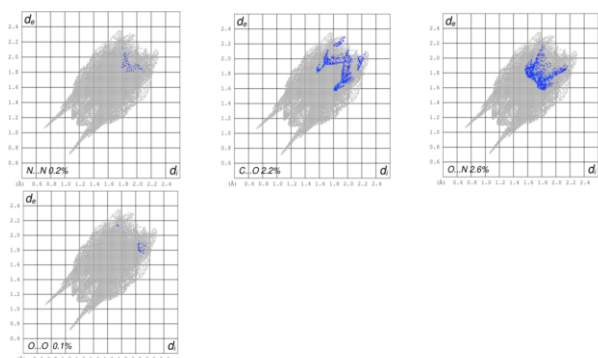


Figure 16. Anhydrous theophylline (I) two-dimensional fingerprint plots with various interaction percentages.

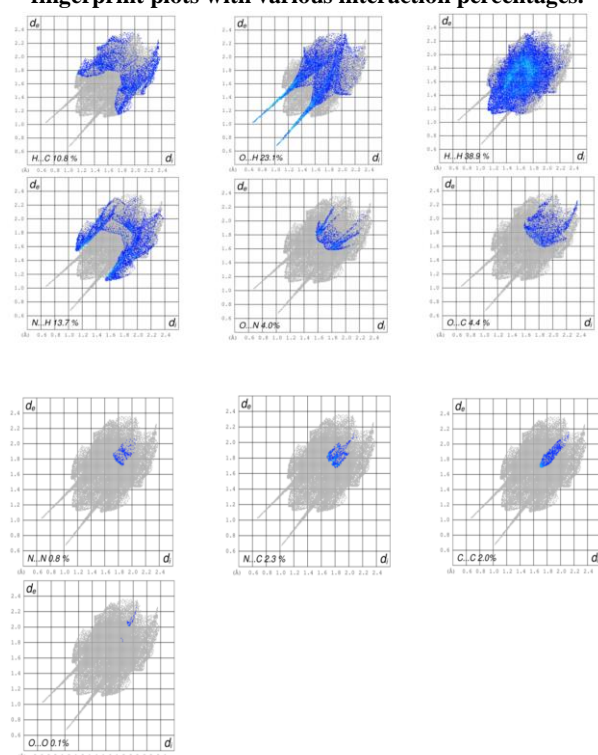


Figure 17. Anhydrous theophylline (II) fingerprint plots.

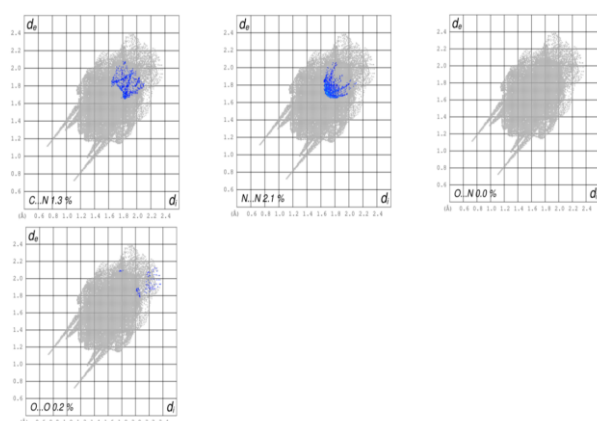
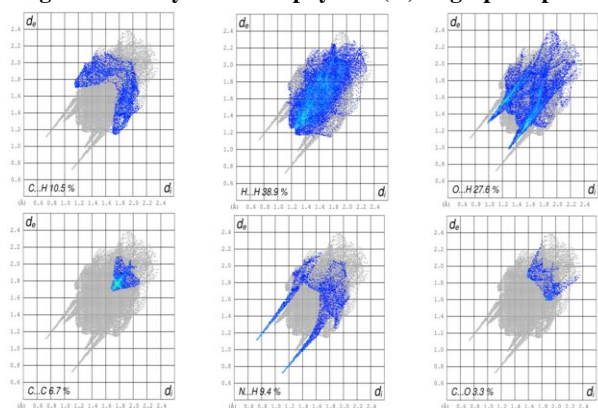


Figure 18. Anhydrous theophylline (III) fingerprint plots.

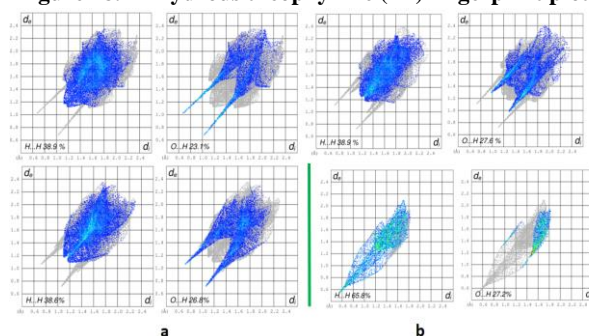
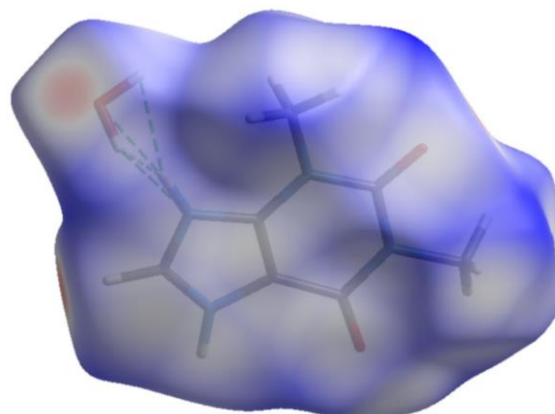


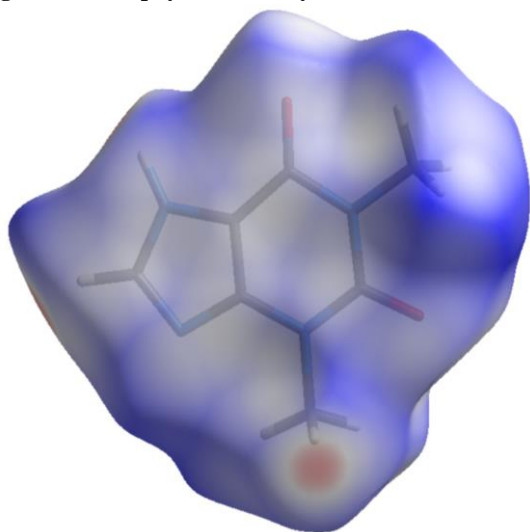
Figure 19 (a) Different polymorphs of anhydrous theophylline have varying percentages of O...H and H...H interactions. (b) O...H and H...H interactions in the water molecule theophylline monohydrate.

Table 5 Comparison of percentage of finger print plots of theophylline monohydrate and anhydrous theophylline

Comparison of percentage of fingerprint plots				
Different types of interactions	Theophylline monohydrate $P2_1/n$	Anhydrous theophylline $P2_1/c$	Anhydrous theophylline $pn$	Anhydrous theophylline $Pna2_1$
H...H	40.9%	38.9%	38.9%	38.6%
O...H	32.5%	23.1%	27.6%	26.8%
H...C	10.0%	10.8%	10.5%	6.8%
O...C	2.1%	4.4%	3.3%	2.2%
O...N	1.8%	4.0%	0.0%	2.6%
N...H	4.3%	3.7%	9.9%	12.7%
C...C	2.2%	2.0%	6.7%	3.2%
N...C	3.6%	2.3%	1.3%	6.9%
N...N	1.2%	0.8%	2.1%	0.2%
O...O	1.5%	0.1%	0.2%	0.1%





**Figure 20. Theophylline monohydrate Hirshfeld surface.****Figure 21. Anhydrous theophylline Hirshfeld surface.**

## Conclusion

From the aforementioned research, we deduced that Hirshfeld interface evaluation is a crucial technique for studying intermolecular interactions and is particularly useful when comparing polymorphic compounds. The Hirshfeld surface assessment supports the intermolecular forces associated with crystal packaging. Recent research has used cutting-edge methods like Hirshfeld surfaces to examine the structure of theophylline monohydrate and polymorphs of dehydrated theophylline. Theophylline hydrate has a lower proportion of intermolecular bonds than anhydrous theophylline because it contains a water component. The proportion of some couplings varies in combinations of anhydrous theophylline, which is supported by fingerprint patterns. Theophylline monohydrate contains H<sub>2</sub>O molecules, which are particularly beneficial for maintaining a crystalline framework. Theophylline monohydrate has improved tablet ability and flexibility because of the water component. Hirshfeld surface and fingerprint graphs are appropriate for comparing the non-covalent bonds that polymorphs exhibit in structures with environments having  $Z > 1$ . The study concluded that the primary intermolecular forces have a significant influence on the crystalline packaging and physicochemical characteristics of theophylline monohydrate and polymorphs of anhydrous theophylline. H-bond varies between polymorphs of anhydrous theophylline crystalline packing owing to differing ratios of certain intermolecular forces.

## References

1. Sun, C.C., *Materials science tetrahedron—A useful tool for pharmaceutical research and development*. Journal of pharmaceutical sciences, 2009. **98**(5): p. 1671-1687.
2. Desiraju, G.R., *Crystal engineering: from molecule to crystal*. Journal of the American Chemical Society, 2013. **135**(27): p. 9952-9967.
3. 3Hiestand, E.N., *Mechanical properties of compacts and particles that control tableting success*. Journal of pharmaceutical sciences, 1997. **86**(9): p. 985-990.
4. Jain, S., *Mechanical properties of powders for compaction and tableting: an overview*. Pharmaceutical Science & Technology Today, 1999. **2**(1): p. 20-31.
5. Spackman, M.A. and D. Jayatilaka, *Hirshfeld surface analysis*. CrystEngComm, 2009. **11**(1): p. 19-32.
6. Bofill, L., et al., *DFT analysis of uncommon  $\pi \cdots H$ -bond array interaction in a new pterostilbene/theophylline cocrystal*. Crystal Growth & Design, 2020. **20**(10): p. 6691-6698.
7. Chang, S.-Y. and C.C. Sun, *Superior plasticity and tabletability of theophylline monohydrate*. Molecular pharmaceutics, 2017. **14**(6): p. 2047-2055.
8. Sun, C., et al., *Theophylline monohydrate*. Acta Crystallographica Section E: Structure Reports Online, 2002. **58**(4): p. o368-o370.
9. OTSUKA, M. and N. KANENIWA, *The dehydration kinetics of theophylline monohydrate powder and tablet*. Chemical and pharmaceutical bulletin, 1988. **36**(12): p. 4914-4920.
10. Rodríguez-Hornedo, N. and H.-J. Wu, *Crystal growth kinetics of theophylline monohydrate*. Pharmaceutical research, 1991. **8**: p. 643-648.
11. Khomane, K.S. and A.K. Bansal, *Effect of particle size on in-die and out-of-die compaction behavior of ranitidine hydrochloride polymorphs*. AAPS PharmSciTech, 2013. **14**: p. 1169-1177.
12. Moulton, B. and M.J. Zaworotko, *From molecules to crystal engineering: supramolecular isomerism and polymorphism in network solids*. Chemical reviews, 2001. **101**(6): p. 1629-1658.
13. Novena, L.M., et al., *Synthesis, crystal structure, hirshfeld surface analysis, spectral and quantum chemical studies of pharmaceutical cocrystals of a bronchodilator drug (Theophylline)*. Journal of Molecular Structure, 2022. **1249**: p. 131585.
14. Bojarska, J. and W. Maniukiewicz, *Investigation of intermolecular interactions in finasteride drug crystals in view of X-ray and Hirshfeld surface analysis*. Journal of Molecular Structure, 2015. **1099**: p. 419-426.
15. Jelsch, C., K. Ejsmont, and L. Huder, *The enrichment ratio of atomic contacts in crystals, an indicator derived from the Hirshfeld surface analysis*. IUCrJ, 2014. **1**(2): p. 119-128.
16. Spackman, M.A. and J.J. McKinnon, *Fingerprinting intermolecular interactions in molecular crystals*. CrystEngComm, 2002. **4**(66): p. 378-392.
17. Allen, F.H., et al., *The Cambridge Crystallographic Data Centre: computer-based search, retrieval, analysis and display of information*. Acta Crystallographica Section B: Structural

- Crystallography and Crystal Chemistry, 1979. **35**(10): p. 2331-2339.
18. Spackman, P.R., et al., *CrystalExplorer: A program for Hirshfeld surface analysis, visualization and quantitative analysis of molecular crystals*. Journal of Applied Crystallography, 2021. **54**(3): p. 1006-1011.
  19. Fucke, K., et al., *New insights into an old molecule: interaction energies of theophylline crystal forms*. Crystal growth & design, 2012. **12**(3): p. 1395-1401.
  20. Spackman, M.A. and P.G. Byrom, *A novel definition of a molecule in a crystal*. Chemical physics letters, 1997. **267**(3-4): p. 215-220.
  21. Fatima, A., et al., *Quantum Chemical, experimental spectroscopic, Hirshfeld surface and molecular docking studies of the anti-microbial drug Sulfathiazole*. Journal of Molecular Structure, 2021. **1245**: p. 131118.
  22. Fatima, A., et al., *Quantum computational, spectroscopic, Hirshfeld surface, electronic state and molecular docking studies on sulfanilic acid: An anti-bacterial drug*. Journal of Molecular Liquids, 2022. **346**: p. 117150.